Available online at www.sciencedirect.com

SCIENCE DIRECT®

Thermochimica Acta 414 (2004) 85–90

thermochimica acta

www.elsevier.com/locate/tca

Studies of structures of poly-ε-caprolactam/montmorillonite nanocomposite

Part 2. Tests of annealed specimens

B. Jurkowski [a,*], Y.A. Olkhov [b]

[a] *Plastic and Rubber Processing Division, Polymer Processing Laboratory, Poznan University of Technology, Piotrowo 3, Poznan 61-138, Poland*
[b] *Institute of the Problems of Chemical Physics, Russian Academy of Sciences, 142 432 Chernogolovka, Moscow Region, Russia*

Received 11 April 2003; received in revised form 17 September 2003; accepted 22 November 2003

Abstract

Using the novel version of thermomechanical analysis (TMA) method, a poly-ε-caprolactam (PA6) and its nanocomposite (PNC) containing 1.6 wt.% of montmorillonite (MMT) were examined. Several disc specimens of those as investigated in the first part of this article were then melted, annealed, and sheared at a rate of $0.5\,s^{-1}$ engendering ca. 140% strain at 240 °C in a rotational rheometer, and next solidified in ambient air. In PNC as in PA6 specimens prepared in the same way, an amorphous isotropic structure in the surface layer up to 0.5 mm thick was identified, with topological regions differing in thermal expansion properties and related a state of order. This finding differs from other tests, which detect a high level of crystallinity. Probably, it is related with small thickness of the tested layer of material and kinetics of solidification in ambient air.

An increase in the free volume fraction, V_f^{TMA}, evaluated as equal to $3\Delta\alpha T_g$ ($\Delta\alpha$ is the difference in linear thermal expansion coefficients below and above the glass transition temperature T_g) and resulted from melting, annealing, shearing, and next solidification in ambient air was observed. It suggests that these operations introduce into the specimen some amount of gases (e.g., evaporated water absorbed when cooling) what increases thermal expansion over high-temperature transition of the high-temperature topological region. It means that V_f^{TMA} is a sum of all voids within a specimen tested (not only a real free volume) independently on their origin. Because of this, it is better to term it as micro or nanoporosity.

Keywords: TMA; PA6; Montmorillonite; Nanocomposite; Topological structure; Molecular structure; Pseudo-network

1. Introduction

Considering the growing importance of polymer nanocomposites (PNC) to the global economy, it is necessary to investigate effective ways for the optimization of their processing technology and testing.

The general motivation for this work was to complement the study of structure and properties of a poly-ε-caprolactam (PA6) nanocomposites. For comparison, two commercial polymers, PA6 and based on it PNC are used. The latter polymer usually contains 2.0 wt.% organoclay or 1.6 wt.% (i.e., 0.64 vol.%) of montmorillonite (MMT) intercalated with ω-amino dodecanoic acid. In the first part of this work [1] a structure of compression molded neat PA6 and based on it PNC have been studied and there is given a literature review of 60 references. Now the aim is to study an influence on the above compression molded material of successive melting, annealing, and shearing at a rate of $0.5\,s^{-1}$ engendering ca. 140% strain at 240 °C in a rotational rheometer, and next cooling in ambient air when some adsorption of water could not be excluded. The work showed a strong interaction between organoclay and PA6 that caused solidification of chains on the platelet surface well above the bulk melting point. This work is based on the novel thermomechanical analysis (TMA) methodology [2].

2. Experimental

2.1. Materials

The two commercial polymers were supplied free of charge by the Ube Industries Ltd. However, information

---

* Corresponding author. Fax: +48-61-6652-217.
E-mail address: boleslaw.jurkowski@put.poznan.pl (B. Jurkowski).

0040-6031/$ – see front matter © 2003 Elsevier B.V. All rights reserved.
doi:10.1016/j.tca.2003.11.022

on properties of the nanoclay used we did not obtain. The specimens as discs were prepared according to following procedures:

The first sample was well dried PA6 (Nylon 1015B $\bar{M}_n = 22\,\text{kg/mol}$, heat deflection temperature HDT $= 75\,^{\circ}\text{C}$ and flexural elastic modulus $E = 285\,\text{MPa}$). It was compression molded in a Carver laboratory press for 5 min at the temperature $T = 235\,^{\circ}\text{C}$ and pressure $P = 70\,\text{MPa}$. Then the press plates were cooled by cold water, pressure release and specimens removed from the mold. Next, specimens were placed in ARES constant strain rate rheometer (Rheometrics). The soak time at 240 °C of 3 min was allowed, and then the molten specimen was sheared between parallel plates (25 mm diameter, gap 1.4 mm) at a steady state shear rate $\dot{\gamma} = 0.5\,\text{s}^{-1}$ (total shear strain at the specimen rim: $\gamma \cong 140\%$). Thus, the specimen deformation was non-uniform: none in center, and maximum at the rim. Next, the heating was switched off, the oven open and the specimen was allowed to cool down in ambient air. The solidification was fast as the crystallization temperature is about 200 °C.

The second sample was well dried PNC (Nylon 1015C2 containing 1.6 wt.% exfoliated clay in PA6 matrix, having $\bar{M}_n = 22\,\text{kg/mol}$). It was compression molded as above. By comparison to neat PA6, the PNC has density a little higher (ca. 1%), heat deflection temperature (HDT) 140 °C increased by 65 °C and higher flexural elastic modulus ($E = 359\,\text{MPa}$, i.e., increased by 26%). Then material was put in rheometer, melted and sheared, and then solidified analogously as specimen #1. According to rheological data given by Utracki (confirmed by the transmission electron microscopy, TEM), this treatment is resulted in alignment of clay platelets in the flow direction.

3. Methodology

The TMA methodology used in this study grounds on a simplified model polymer network with physical junctions and/or chemical crosslinks and testing polymers at solid and visco-elastic states. The methodology of measurements and, next, basing on the obtained results, evaluation of the molecular weight distribution (MWD) of chain segments between the junctions of the network (or pseudo-network) in each topological region (confirmed experimentally on model networks), a crystallinity degree, and shares of amorphous topological regions with different thermal properties are described in detail elsewhere [2]. The theories on which the TMA is based [3,4] and co-ordinates of transitional zone on the thermomechanical curve (TMC) suggest similarity of a segment of the TMC with the integral curve of the MWD from the GPC data for polymers. We termed this segment a pseudo-integral curve because the integral MWD curve can be drawn when all shares of particular fractions and their molecular weights have been calculated. It means that in this way could be calculated MWD of the polymer in a solid state. Its value is different from GPC because of differences in testing conditions. The obtained parameters of molecular and topological structures correlate satisfactory with the mechanical properties of cured rubbers [5–7] and are not contradictory with the NMR [8] and swelling experiments [9].

The specimens cut from fabricated parts give response that depends on the distance from the surface and orientation, viz. in machine direction (MD) or parallel to stress (II) and in transverse direction (TD) or perpendicular to stress (⊥) what should give some information on influence of processing conditions on material structure at layer up to 0.5 mm thick. Some of such measurements were performed in this study.

4. Results and discussion

4.1. Effect of PA6 additional melting, annealing, and shearing

Shearing stresses applied by rheometer during twisting of molten, previously compression molded polymer are directed under some angle against vectors of streams flowing in the mold. This destroys polymer structure formed previously during molding. The test specimen was removed from the rheometer oven at 240 °C and cooled in ambient air until room temperature. This reduces fast the segmental mobility of chain segments between junctions on the specimen surface because this surface is quickly solidified. Heat transfer from a polymer to surrounding air starts immediately after removing it from rheometer, but is different from this in previous experiments [1] when specimen was cooled by water in the mold. in the latter case some thermal inertia takes place due to large heat capacity of the mold. Because of this, when thin layer on a surface is already solidified by surrounding air in discussed here experiment, the inner part of the specimen is still under condition of its crystallization. Therefore, further crystallization could run there giving a gradient of structure. Because of this, one can expect preserving an amorphous or predominantly amorphous structure of thin “skin” layer and creation of semi-crystalline one inside the specimen.

Fig. 1 shows TMC of PA6 specimen processed according to described above procedure and tested in machine direction MD^{II} that is in the direction of compression at molding hence transverse to the shearing direction. The TMA data show that after melting, annealing, shearing, and cooling in ambient air, a surface layer of PA6 up to 0.5 mm thick (this layer is virtually tested by TMA) is predominantly amorphous, but with two topological regions differing in thermal expansion properties. For the compression-molded specimen described previously [1], it was postulated that the pseudo-network was formed predominantly by physical junctions of crystallites and some other junctions like clusters, or chain entanglement. However, a crystalline fraction is not detected now by TMA on a surface of PA6 specimen of the same composition as previously, but junctions of a pseudo-network still exist. In the absence of crystallites,

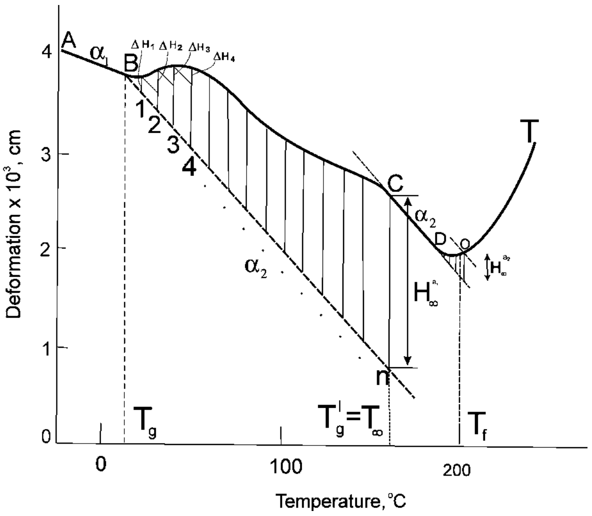

Fig. 1. The thermomechanical curve for melted, annealed, sheared and solidified PA6 tested in MD^{II}.

one must assume formation of substantial amount of micro crystallites or hydrogen-bonded clusters both postulated as not detectable by TMA (as it was suggested earlier by Shershnev [10]), but responsible for the junctions, or chain entanglement. The zone of thermal stability is shown as a high-elasticity plateau (the straight line CD). In this zone the polymer expands with the coefficient of linear thermal expansion $\alpha_2 = 3.15 \times 10^{-4}$ degree^{-1}. Its ratio to α_1 is 4.07, thus in the typical range for amorphous polymers [11].

At the temperature marked by point C, the segmental relaxation of cluster type junctions begins the high-temperature transition in the high-temperature amorphous region ($T_{htt} = 169\,°C$). The lowest-molecular weight PA6 chains start to flow at temperature corresponding to point D.

Simultaneously, an essential increase in thermal expansion at high elastic state and the free volume fraction, V_f^{TMA}, evaluated as equal to $3\Delta\alpha T_g$ ($\Delta\alpha$ is the difference in linear thermal expansion coefficients below and above the glass transition temperature T_g) and resulted from processing and annealing was observed. Why it happens? This fact could be explained as follows: polyamide is a hygroscopic material. Because of this, during cooling from 240 °C in ambient air until room temperature, the PA6 can absorb some water, which will be located in its amorphous (less compact) region. During further TMA test, when temperature raises much over T_g, evaporating of this water should increase expansion of specimen. As a result, the value the linear thermal expansion coefficient above the glass transition temperature, α_2, and resulting V_f^{TMA} now are overestimated in comparison with those for dry material. This suggests that these technological operations have introduced into the specimen some amount of additional voids. It means that in the tested case, $V_f^{TMA} = 3\Delta\alpha T_g$ is not the free volume fraction, as accepted by some scientists [12–14], but a sum of all voids within the specimen tested independently on their origin. Because of this, it could be named as compaction factor V_c^{TMA} and could be a measure of micro or nano porosity.

The PA6 specimen was also tested in transverse direction $TD^{\perp}$ regime. However, the TMC in both test directions (II) and ($\perp$) were similar, suggesting virtually an isotropic structure of molten, annealed, sheared, and cooled in ambient air PA6 (see Table 1). From the T_g values, linear thermal expansion coefficients and the free volume fractions, one may conclude that in PA6 specimen there are only minor differences due to orientation within the low-temperature amorphous region. This suggests that melting, annealing, shearing, and further slow cooling in ambient air of the specimen at conditions of our experiments makes a structure of PA6 isotropic, which previously (after compression molding) was anisotropic. It was obtained from 3 to 5 parallel tests and annealing at 100–120 °C what melt the existing 67 wt.% of crystalline portion characterized by temperature of the beginning of melting $T_m = 46\,°C$. This melting should result in virtually full rendering amorphous polymer.

4.2. *Effect of MMT introduction, additional melting, annealing, and shearing*

The formulation of PNC specimen is identical to that described in work [1], but after compression molding, the specimen was next melted, annealed, and sheared to impose some orientation, and cooled in ambient air until room temperature as above for neat PA6. The used additive (montmorillonite) is hygroscopic. Because of this, all phenomena related with absorption and desorption of water discussed above for PA6 should be present also here, but more intensive. One should remember also that a cooling rate for inner part is now lower and for a surface is higher than those for PNC compression molded specimen tested in work [1] what should be reflected in a gradient of material structure. The chain segments between junctions in a pseudo-network at $T_{htt} \leq T \leq T_g$ (Table 1) display substantial anisotropy in packing density in both a glassy and in an elastic state (compare α_1 and α_2 for different orientation). However, some changes in average molecular weight of amorphous portion and crosslinking degree have been observed, what suggest that melting, annealing, and shearing have degraded some portion of junctions in a pseudo-network of PNC, which could be transformed into another structure. Cooling in air promotes solidification of amorphous material, especially in a surface layer, what all above taken together gives a substantial lowering of equilibrium elastic modulus and supports above conclusion.

The TMC for PNC specimen shown in Fig. 2 is virtually identical to that for Fig. 1, but shifted to higher temperatures by ca. 18 °C, what could be related with interaction of MMT platelets with polymer chains. Molecular weight and relaxation characteristics of its topological structure with two amorphous regions evaluated in both test directions are listed in Table 1. From these data, it appears that an isotropic character of topological structure is accompanied by anisotropy of changes in molecular mobility of the chain segments

Table 1
Molecular and topological structures of PA6 and its nanocomposite (PNC) melted, annealed, sheared, and cooled in ambient air

Analyzed parameter[a] (95% confidence limit)	PA6 II[b]	$\perp$[b]	PNC II	$\perp$
Low-temperature amorphous region				
T_g (°C (±3–5))	14	−30	32	−19
$\alpha_1 \times 10^5$ (degree^{-1} (±10%))	7.7	3.7	8.5	3.0
$\alpha_2 \times 10^5$, (degree^{-1} (±10%))	31.45	21.5	38.8	12.8
V_f^{TMA} (±10%)	0.204	0.126	0.277	0.075
$\bar{M}'_w$ (kg/mol (±10%))	25.8	57.9	24.0	29.6
K' (±10%)	1.55	1.74	1.51	1.69
E_∞ (MPa (±10%))	0.72	0.80	1.03	0.70
$\upsilon_e \times 10^4$ (±10%)	0.66	0.73	0.94	0.63
φ' (±10%)	0.88	0.84	0.63	0.90
High-temperature amorphous region				
T_{htt} (°C (±3–5))	160	160	159	165
V_f^{TMA} (±10%)	0.307	0.231	0.393	0.129
$\bar{M}''_w$ (kg/mol (±10%))	33.4	22.9	631	316
K'' (±10%)	2.29	1.99	1.59	1.00
T_f (°C (±3–5))	200	203	203	206
φ'' (±10%)	0.12	0.16	0.37	0.10
Values averaged between regions[c]				
$\bar{M}_w$ (kg/mol (±10%))	26.0	25.8	1340	58.3
K (±10%)	1.59	1.80	54.5	3.0

[a] $K = \bar{M}_w/\bar{M}_n$, polydispersity index; $\bar{M}_w$, the weight–average molecular weight; $\bar{M}_n$, the number–average molecular weight; T_f, temperature of the beginning of molecular flow; T_g, the glass transition temperature; T_{htt}, temperature of the high temperature transition; V_f^{TMA}, the free volume fraction calculated as $3\Delta\alpha T_g$; α_1, the coefficient of linear thermal expansion in a glassy state; α_2, the coefficient of linear thermal expansion in a high-elastic state, low-temperature region; φ', a weight share of a low-temperature amorphous region; φ'', a weight share of a high-temperature amorphous region.

[b] Orientation in machine direction (MD) or parallel to stress (II) and in transverse direction (TD) or perpendicular to stress ($\perp$).

[c] Averaging was performed using weight shares of the regions and respective $\bar{M}_w$ magnitudes.

between junctions in the low-temperature amorphous region (changes in T_g and V_f^{TMA}) and its weight share φ. In addition, parameters characterizing density of molecular packing of the chains in glassy and high-elastic states are anisotropic (changes in α_1 and α_2). Relations between evaluated characteristics for PNC specimen are analogous to that for PNC compression molded specimen discussed in work [1].

The high molecular weight chains in PNC are in a solid state up to about 160 °C, Fig. 2. Most likely, MMT/polymer complexes act there as polyfunctional branching junctions and participate in the resistance to outer loading applied to solid body. Here the chemical structure of chain segments between the junctions in a pseudo-network could play also the principal role in properties of a low-temperature amorphous region, especially under impact. If it is true, an influence of nanofiller and compounding as well as processing procedures on a structure of PNC disappears if shear stresses, especially at high temperature, are applied. At these conditions, MMT/polymer physical junctions are degraded. However, another junctions should be formed after termination of shear and thermal fields' action. Similar conclusion could be made for mentioned above results of PA6, which also after annealing and shearing became isotropic.

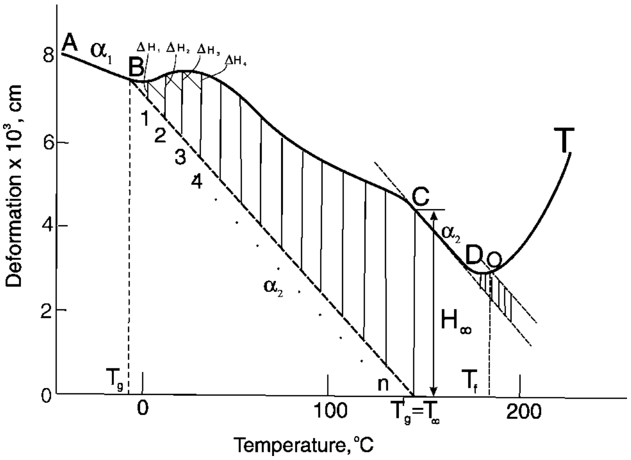

Fig. 2. The thermomechanical curve for melted, annealed, sheared and solidified PNC tested in MD$^{\mathrm{II}}$.

Melting, annealing, shearing, and next cooling in ambient air influences a structure of high-temperature amorphous region of PNC specimen in slightly different way (see changes in V_f^{TMA}) than that for PA6. The latter specimen was found to be fully isotropic (the same high transition temperature T_{htt} in both regimes of testing) while in PNC some anisotropy in packing density of the chain segments is observed ($T_{\mathrm{htt}}^{\mathrm{II}} = 159$ °C and $T_{\mathrm{htt}}^{\perp} = 165$ °C). Most likely, it is resulted from MMT platelets' orientation, but this difference is in the zone of statistical scatter of evaluation the transition temperature. Simultaneously, an essential increase in V_f^{TMA} resulted from melting, annealing, shearing, and next cooling in ambient air was observed, what suggests that conclusion above from T_{htt} is true. This suggests also that these technological operations introduce into the specimen some amount of gases

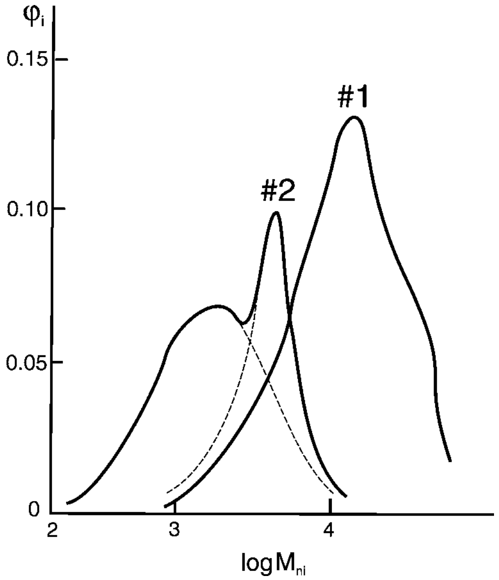

Fig. 3. Molecular weight distributions (MWD) of the chain segments between junctions in amorphous pseudo-networked portion for PA6 and PNC (specimen #1 and 2, respectively) tested in $\mathrm{MD}^{\mathrm{II}}$.

or liquids evaporating at testing conditions what increases thermal expansion at temperatures over T_{htt}. It means that $V_{\mathrm{f}}^{\mathrm{TMA}}$ in both the tested case and that described in article [1] are a sum of all voids within a specimen (not only a real free volume) independently on their origin as it was concluded above for PA6.

Concentrations of the chain segments between junctions (ν_{e}) in a pseudo-network of amorphous regions (see Table 1) are stable for every polymer and polymer composite at temperatures from T_{∞} (temperature of the beginning of a plateau of high-elasticity) to the temperature of next relaxation transition. For compression molded neat both PA6 and PNC specimens given in [1] it is T_{m}' (they have crystalline portion), when for the same material but melted for the second time, annealed, sheared, and cooled in ambient air (current investigation) it is T_{g} because of a lack of crystalline portion in a surface layer.

E_{∞} in the zone of thermal stability of a pseudo-network depends only on temperature. Its minimum is reached for neat PA6 and PNC at T_{m}' [1], but for processed and annealed PA6 specimen and PNC specimen discussed in this article is at T_{g} (Table 1). This Table also shows that E_{∞} depends on orientation of measuring probe against specimen surface.

4.3. Changes in MWD between junctions

The molecular weight distribution of the chain segments between junctions of a pseudo-network at low-temperature amorphous region for PA6 and PNC, Fig. 3, is similar, but not identical in character, It is bimodal for PNC (curve 2) and monomodal for PA6 (curve 1), but with some bending of the MWD right branch. This observation suggests to assume both of them as combined of two MWD with similar low and high-molecular weight components of spectrum of chain length. Based on these facts, it could be assumed preliminarily that pseudo-networks in both PA6 and PNC could be two different kinds of branching junctions.

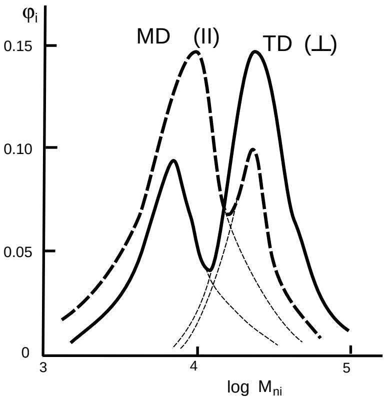

Fig. 4. Molecular weight distributions (MWD) of the chain segments between junctions in amorphous pseudo-networked portion for annealed and sheared PNC tested in $\mathrm{MD}^{\mathrm{II}}$ and $\mathrm{TD}^{\perp}$.

In $\mathrm{MD}^{\mathrm{II}}$ and $\mathrm{TD}^{\perp}$, the character of MWD in PNC (Fig. 4) is virtually the same—bimodal, but with different weight shares of low and high molecular weight components of spectrum of chain length.

Introduction of MMT substantially increases molecular weight in the intermediate and high-melting crystalline portion detected in $\mathrm{MD}^{\mathrm{II}}$ (Table 1). It is expected that the high-molecular weight fractions of PA6 are easier to orient under stress applied than the low-molecular ones. Furthermore, such orientation should be perpendicular to the vector of compression stresses, as it was observed for specimens tested in $\mathrm{MD}^{\mathrm{II}}$.

An effect of high molecular weight fractions of PA6 in PNC tested in $\mathrm{TD}^{\perp}$ was not evident. This may be explained by a fact that the main component of thermal expansion of PNC specimen at melting of the chain segments included in crystalline portion and devitrification of those being in a glassy state acts at different direction from possible recording in the testing device. It is believed that this phenomenon is the reason for an existence of different magnitudes of $\bar{M}_{\mathrm{w}}$ evaluated at different test directions (Table 1).

5. Conclusions

Procedure of specimens manufacturing when melting, annealing, and shearing take place could form the spatially isotropic amorphous topological structure on a surface of PA6 if it is solidified in ambient air. Based on molecular weights in topological regions and their weight shares from TMA tests one can calculate an average magnitude close to that obtained by independent measurements using other methods.

An essential increase in free volume fraction $V_{\mathrm{f}}^{\mathrm{TMA}}$ evaluated as equal $3\Delta\alpha T_{\mathrm{g}}$ and resulted from melting, annealing, shearing, and next cooling in ambient air was observed, what suggest that these technological operations introduce into the specimen some amount of gases or liquids (e.g., evaporating water absorbed when cooling in ambient air) what increases thermal expansion at temperatures over T_{htt}. It means that $V_{\mathrm{f}}^{\mathrm{TMA}}$ is a sum of all voids within a specimen tested (not only a real free volume having a size in Ångstrems) independently on their origin. Because of this, it is better to term it as micro or nanoporosity.

Discussion above supports our previous conclusion about usefulness of TMA to obtain some supplementary information about polymer structure.

Acknowledgements

L.A. Utracki from NRCC/IMI in Canada supplied the specimens used in this work. We are very obliged for his fruitful discussion. The authors thank the Polish State Committee of Scientific Research (Grant 4 TO8E 067 25) for financial support.

References

[1] B. Jurkowski, Y.A. Olkhov, Thermochim. Acta (submitted for publication, first part of this article).
[2] B. Jurkowska, Y.A. Olkhov, B. Jurkowski, J. Appl. Polym. Sci. 74 (1999) 490.
[3] Y.A. Olkhov, Y.I. Estrin, SU Patent 154,0463 (July 3, 1987).
[4] Y.A. Olkhov, S.M. Baturin, V.I. Irzhak, Polym. Sci. (Russia) A 38 (5) (1996) 849.
[5] B. Jurkowski, B. Jurkowska, Elastomery (PL) 6 (4/5) (2002) 3–11.
[6] B. Jurkowska, B. Jurkowski, C. Nah, Elastomer (Korea) 37 (4) (2002) 234–243.
[7] B. Jurkowska, B. Jurkowski, J. Appl. Polym. Sci. 90 (9) (2003) 2583–2591.
[8] B. Jurkowski, Y.A. Olkhov, B. Jurkowska, H. Menge, Polym. Test. 21 (5) (2002) 597–606.
[9] B. Jurkowska, B. Jurkowski, Y.A. Olkhov, Kautschuk Gummi Kunststoffe (submitted for publication).
[10] V.A. Shershnev, I.K. Shundrina, V.D. Yulovskaya, Y.B. Evreinov, Kauchuk i Rezina 1 (1997) 16.
[11] B. Jurkowski, B. Jurkowska, K. Andrzejczak, Polym. Test. 21 (2) (2002) 135.
[12] R.F. Boyer, Rubber Chem. Technol. 36 (1963) 1303.
[13] Y.S. Lipatov, Uspiekhi Khimii 47 (2) (1978) 332.
[14] V.P. Privalko, Molecular structure and properties of polymers, Khimia, Leningrad, 1986 (in Russian).